Effect of structural parameters of Gaussian repaired pit on light intensity distribution inside KH_2PO_4 crystal*

Xiao Yong(肖 勇)[a], Chen Ming-Jun(陈明君)[a]†, Cheng Jian(程 健)[a], Liao Wei(廖 威)[b], Wang Hai-Jun(王海军)[b], and Li Ming-Quan(李明全)[a]

[a] *Center for Precision Engineering, Harbin Institute of Technology, Harbin* 150001, *China*
[b] *Chengdu Fine Optical Engineering Research Center, Chengdu* 610041, *China*

(Received 23 October 2013; revised manuscript received 20 February 2014; published online 10 June 2014)

KH_2PO_4 (KDP) crystal with excellent optical properties is a very important element of inertial confinement fusion (ICF) device. However, KDP crystal surface micro-defects severely reduce the crystal laser damage threshold, affecting the crystal service life. In this paper, Gaussian repaired pit is used to replace the crystal surface micro-defects, in order to improve the laser damage resistance of the KDP crystal with surface micro-defects. At first, the physical model of Gaussian repaired pit is built by Fourier model method, and the accuracy of the method is analyzed. It is found that the calculation error can be reduced by increasing the product of the width–period ratio and the truncation constant of the repaired pit. The calculation results about the physical model of Gaussian repaired pit show that the light intensity distribution within the crystal is symmetrical, and there are evidently enhanced light intensity regions in the crystal. Meanwhile, the maximum relative intensity inside the KDP crystal decreases gradually with the increase of the width of the Gaussian repaired pit. Secondly, the Gaussian repaired pits with different widths and the same depth of 20 μm are processed by micro-milling. Their surfaces are very smooth and present the ductile cutting state under the microscope. Finally, the laser damage threshold of the Gaussian repaired pits on the surface of the KDP crystal sample is measured by a 3ω, 6-ns laser. The results show that the maximum threshold of the Gaussian repaired pits is 3.12 J/cm^2, which is 60% higher than the threshold of initial damage point, and the laser damage threshold increases with the increase of the width of the Gaussian repaired pit.

Keywords: KH_2PO_4, Gaussian repaired pit, Fourier modal method, laser damage threshold

PACS: 77.84.Fa, 42.60.Jf, 02.30.Nw, 42.70.Mp **DOI:** 10.1088/1674-1056/23/8/087702

1. Introduction

Energy shortage receives the world's attention, and the inertial confinement fusion (ICF) provides a solution to the problem.[1,2] KDP crystal has excellent optical properties and can grow to a large size, so it is a very important optical component, used as an optical frequency doubling crystal and optical switching transistor in an ICF device.[3–5] However, during the ultra-precise machining and high energy laser irradiation, small defects, such as crack, ablation, melting, etc., may occur on the surface of KDP crystal.[6,7] These initial defects would grow rapidly at following laser irradiation, and they greatly reduce the laser damage threshold of KDP crystal and shorten the life of the crystal component.

The recent studies showed that the initial defects can be replaced by smooth pits by means of micro-machining, which can effectively improve the laser damage resistance of KDP crystal. Guillet *et al*. processed that small ball pits on the surface of KDP crystal should be repaired by micro-grinding, and this method could alleviate the growth of initial damage.[8] Geraghty *et al*. used the machined Gaussian and conical repaired pits instead of the initial defects, which could significantly improve the laser damage threshold of KDP crystal with initial defects.[9] Moreover, the research into microstructures on the surface of KDP crystal affecting the laser damage resistance, hasfocused on micro-waves, micro-cracks, etc. For example, Li *et al*. investigated how the micro-waves on the surface of KDP crystal, produced during processing by means of single point diamond turning, influence the laser damage threshold of KDP crystal.[10] Cheng *et al*. studied how the micro-cracks affect the light intensity modulation inside KDP crystal, by the finite difference time domain (FDTD) method.[11] However, the sizes of repaired pits produced by means of micro-machining method also have an important influence on the laser damage threshold of KDP crystal, which has rarely been reported so far.

In this paper, the Gaussian repaired pits processed by micro-milling method are simplified into perfect Gaussian curves. The physical model of Gaussian repaired pit is built by Fourier model method, and the paper investigates how the Gaussian repaired pits with different widths and depths affect the light intensity modulation inside KDP crystal. Then, a micro-precise five-axis machine tool is used to fabricate the Gaussian repaired pits with different widths on the surface of

*Project support by the National Natural Science Foundation of China (Grant No. 51275113) and the National Science and Technology Major Project of China (Grant No. 2013ZX04006011-215).

†Corresponding author. E-mail: chenmj@hit.edu.cn

© 2014 Chinese Physical Society and IOP Publishing Ltd

KDP crystal sample piece, and the laser damage threshold of these repaired pits were measured experimentally. These efforts can provide a theoretical basis for repairing the surface defects on the large diameter KDP crystal components.

2. Model and theory

To improve laser damage resistance, Gaussian repaired pits are substituted for the initial laser-induced damage spots on the surface of KDP crystal. Generally, the size of initial damage spot could be beyond dozens of microns,[12] for which the traditional finite element method is not suitable. Therefore, the Fourier model theory with rigorous electromagnetic field analysis is used to compute the incident laser modulation caused by Gaussian repaired pits.[13–15] The ideal geometric form of Gaussian repaired pit is a part of Gauss surface as shown in Fig. 1.

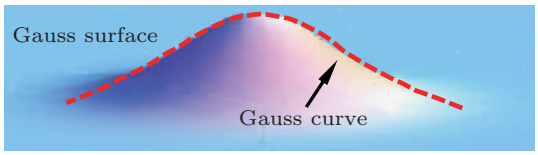


Fig. 1. (color online) Repaired pit of Gaussian shape.

2.1. Physical model of Gaussian repaired pit

Fourier model method is usually used for grating diffraction problem. In order to calculate the laser modulation of repaired pits, simplified model is built in this paper. Firstly, a three-dimensional (3D) Gauss surface is simplified into a two-dimensional (2D) Gauss curve. Then, a kind of particular grating is used to approximate the single repaired pit. In the following section, numeric calculation model of Gaussian repaired pit is built.

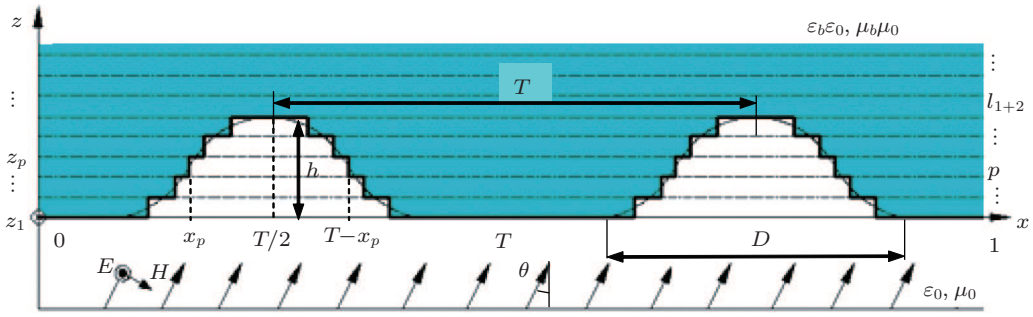


Fig. 2. (color online) Physical model of repaired pit of Gaussian shape.

Physical model of Gaussian repaired pit is shown in Fig. 2. The width of Gaussian repaired pit is D, the depth is h, and the period of physical model is T. The Gaussian curve satisfies the following equation:

$$z = h\exp\left\{-2(x-\frac{T}{2})^2/\omega^2\right\}\cdots x\in\left[\frac{T-D}{2},\frac{T+D}{2}\right],\quad z\geq 0, \tag{1}$$

where ω is equal to $D/3$. In the x–z plane, the first quadrant is KDP crystal, and the fourth quadrant is atmosphere. The first and the (l_1+l_2+2)-th layers are the incident and emergent air layer, respectively. The second-to-the-(l_1+1)-th layers are the repaired pit layers, and the (l_1+2)-th-to-the-(l_1+l_2+1)-th layers are the substrate layers. The angle between direction of incident laser and the z axis is θ, the directions of electric field and magnetic field are shown in Fig. 2.

In the p-th layer, the length of rectangle is the corresponding width of the x direction as the depth of repaired pit is equal to $(z_p+z_{p-1})/2$. The x-coordinate of boundaries is x_p and $T-x_p$ respectively for the p-th rectangle, the mathematical expressions are

$$\begin{cases} x_p = \dfrac{1}{2}T - \dfrac{D}{3}\sqrt{-\dfrac{1}{2}\ln\dfrac{z_p+z_{p-1}}{2h}}, \\ T-x_p = \dfrac{1}{2}T + \dfrac{D}{3}\sqrt{-\dfrac{1}{2}\ln\dfrac{z_p+z_{p-1}}{2h}}. \end{cases} \tag{2}$$

The relative dielectric constant $\varepsilon(x)$ and relative permeability $\mu(x)$ in the p-th layer are given as follows:

$$\varepsilon(x)^p, \mu(x)^p = \begin{cases} \varepsilon_b, \mu_b, & x\in(0,x^p)\cup(T-x^p,T), \\ 1, & x\in(x^p,T-x^p), \end{cases} \tag{3}$$

where ε_b and μ_b are the relative dielectric constant and relative permeability in substrate layer respectively.

The electromagnetic field of the p-th layer is expressed in the form of Fourier model as

$$[\boldsymbol{E},\sigma\boldsymbol{H}]^p = \exp(\mathrm{i}k_0\alpha_m x)[e_{xm}e_{ym}e_{zm}, -h_{xm}h_{ym}h_{zm}]^p \times \exp[\mathrm{i}k_0\gamma^p(z-z^p)], \tag{4}$$

where α_m is the x component of wave number, $\alpha_m=\alpha_0+\lambda m/T$; m is the series of Fourier model, $m=0,\pm1,\pm2,\ldots,\pm M,\ldots$; k_0 is the wave number; γ_p is an unknown number,

which relates to the z component of wave number in the p-th layer.

In order to compute the eigenmode field inside the KDP crystal, the Fourier expansion of Maxwell equations is performed. However, the dielectric constant and permeability in the x direction are not continuous in the repaired pit layers. The matrix elements of ε, $\bar{\varepsilon}$, μ, $\bar{\mu}$ are expressed respectively as

$$\begin{cases} \varepsilon_{mn} = \dfrac{1}{T}\displaystyle\int_0^T \varepsilon(x)\exp\left[-\mathrm{i}\frac{2\pi}{T}(m-n)x\right]\mathrm{d}x, \\ \bar{\varepsilon}_{mn} = \dfrac{1}{T}\displaystyle\int_0^T \frac{1}{\varepsilon(x)}\exp\left[-\mathrm{i}\frac{2\pi}{T}(m-n)x\right]\mathrm{d}x, \end{cases} \tag{5}$$

$$\begin{cases} \mu_{mn} = \dfrac{1}{T}\displaystyle\int_0^T \mu(x)\exp\left[-\mathrm{i}\frac{2\pi}{T}(m-n)x\right]\mathrm{d}x, \\ \bar{\mu}_{mn} = \dfrac{1}{T}\displaystyle\int_0^T \frac{1}{\mu(x)}\exp\left[-\mathrm{i}\frac{2\pi}{T}(m-n)x\right]\mathrm{d}x, \end{cases} \tag{6}$$

where $m, n = 0, \pm1, \pm2, \ldots, \pm M, \ldots$.

Considering the boundary conditions in the x direction, the Maxwell equations are expanded with the principle of inverse rule which is given by Li.[13] The equations (the superscript p is omitted) are

$$\begin{cases} \bar{\mu}e_y\gamma = h_x, \\ e_x\gamma - \alpha e_z = \mu h_y, \\ \alpha e_y = \mu h_z, \end{cases} \quad \text{and} \quad \begin{cases} -\bar{\varepsilon}h_y\gamma = e_x, \\ h_x\gamma + \alpha h_z = \varepsilon e_y, \\ \alpha h_y = -\varepsilon e_z, \end{cases} \tag{7}$$

where ε, $\bar{\varepsilon}$, μ, $\bar{\mu}$ are $2M+1$ order matrix; e_x, e_y, e_z, h_x, h_y, h_z are $(2M+1)\times 1$ order matrix; α is $2M+1$ order matrix. The eigenvalue equations of TE wave and TM wave can be expressed as

$$\begin{aligned} &\text{TE}: \quad \left(\varepsilon - \alpha\mu^{-1}\alpha\right)e_y = \bar{\mu}e_y\gamma^2, \\ &h_x = \bar{\mu}e_y\gamma, \quad h_z = \mu^{-1}\alpha e_y, \end{aligned} \tag{8}$$

$$\begin{aligned} &\text{TM}: \quad \left(\mu - \alpha\varepsilon^{-1}\alpha\right)h_y = \bar{\varepsilon}h_y\gamma^2, \\ &e_x = \bar{\varepsilon}h_y\gamma, \quad e_z = \varepsilon^{-1}\alpha h_y. \end{aligned} \tag{9}$$

The eigenvalue equations of TE wave and TM wave are dependent on each other in a similar form. Therefore, of the two kinds of waves, only one needs to be discussed. The eigenvalue equation of TE wave is solved in detail below.

Let $\psi = \bar{\mu}^{-1}\left(\varepsilon - \alpha\mu^{-1}\alpha\right)$, then equation (8) will be expressed as

$$\psi e_y = e_y\gamma^2. \tag{10}$$

The $4M+2$ eigenvalue γ and $2M+1$ eigenvector e_y are obtained by solving Eq. (10) (the generalized eigenvalue equation). Particularly, the eigenvalue γ comes in a pair, where $+\gamma$ means the up-going wave and $-\gamma$ refers to the down-going wave. Each eigenvector e_y corresponds to two eigenvalues $(\pm\gamma)$.

The relative dielectric constant $\varepsilon(x)$ and relative permeability $\mu(x)$ are constant in the incident and substrate layers. Therefore, the expressions of eigenvalue and eigenvector are obtained easily in these layers as follows.

In the incident layer ($p = 1$),

$$\gamma_m^1 = \pm\sqrt{1-\alpha_m^2}, \quad e_y^1 = I, \quad h_x^1 = \gamma^1. \tag{11}$$

In the substrate layers ($p = l_1+1, l_1+2, \ldots, l_1+l_2+1$),

$$\gamma_m^p = \pm\sqrt{\varepsilon_b\mu_b - \alpha_m^2}, \quad e_y^p = I, \quad h_x^p = \gamma^p. \tag{12}$$

When eigenmode field is obtained in each layer, the general solution of the mode field is composed of the linear superposition of these eigenmode fields. In the p-th layer, electric field E_y^p and magnetic field H_x^p are expressed as

$$\begin{cases} E_y^p = \exp(\mathrm{i}k_0\alpha x)\,e_y^p \times \{\exp[\mathrm{i}k_0\gamma^p(z-z^p)]\,u^p \\ \qquad + \exp[-\mathrm{i}k_0\gamma^p(z-z^p)]\,d^p\}, \\ \sigma H_x^p = -\exp(\mathrm{i}k_0\alpha x)\,h_x^p \times \{\exp[\mathrm{i}k_0\gamma^p(z-z^p)]\,u^p \\ \qquad - \exp[-\mathrm{i}k_0\gamma^p(z-z^p)]\,d^p\}, \end{cases} \tag{13}$$

where u^p and d^p are column vectors which consist of amplitude coefficients of eigenmode fields for up-going wave and down-going wave respectively. Furthermore, u^p and d^p can be solved by the reflection transmission coefficient matrix (RTCM) algorithm.[16,17]

An electromagnetic wave contains energy which is expressed by the time average of energy flux density. The time average of Poynting vector $\boldsymbol{S}$ is called light intensity I which is expressed as

$$I = \frac{1}{\tau}\int_0^\tau \boldsymbol{S}\mathrm{d}t = \left|\frac{1}{\tau}\int_0^\tau \boldsymbol{E}\times\boldsymbol{H}\mathrm{d}t\right| = \frac{1}{2}\left|\mathrm{Re}\left[\boldsymbol{E}\times\boldsymbol{H}^*\right]\right|, \tag{14}$$

where τ is the response time of photo-detector; $\boldsymbol{H}^*$ is the conjugate complex vector of $\boldsymbol{H}$.

The light intensity inside the KDP crystal is unevenly distributed as its crystal surface has Gaussian repaired pits. The relative light intensity I_R is defined as

$$I_\mathrm{R} = \frac{I}{I_0}, \tag{15}$$

where I_0 is the light intensity inside the crystal with its surface being complete; I is the light intensity at any point inside the crystal with its surface having repaired pits.

The maximal relative light intensity $I_{\mathrm{R}\max}$ is defined as

$$I_{\mathrm{R}\max} = \frac{I_\max}{I_0}, \tag{16}$$

where $I_\max$ is the maximal light intensity inside the crystal.

2.2. Accuracy analysis of model

In fact, the repaired pit on the surface of KDP crystal is nonperiodic. Width–period ratio is defined by $T_\mathrm{r} = T_1/T$, where T_1 is the width of Gaussian repaired pit and T is the period of physical model. The width–period ratio of realistic

repaired pit is infinite. Theoretically, the bigger the width–period ratio, the better approximate effect the physical model could have. In order to reduce the computing error, the truncation constant (M) must be enlarged as the width–period ratio is very large. However, overlarge truncation constant would lead to heavy computation. Therefore, the width–period ratio and truncation constant must be selected carefully.

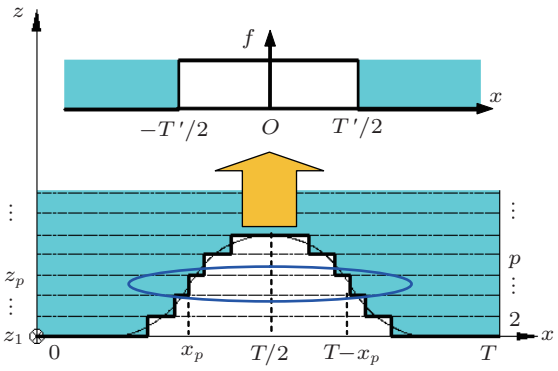


Fig. 3. (color online) Monolayer analysis of physical model.

In the p-th layer, the approximate curve is a window function with period T and width $T-2x_p$ as shown in Fig. 3. In particular, the function of the second layer can be expressed as

$$f(x)=\begin{cases}1, & |x|\le\dfrac{D}{2},\\ 0, & \dfrac{D}{2}\le|x|\le\dfrac{T}{2}.\end{cases} \tag{17}$$

The Fourier expansion of Eq. (17) is expressed as

$$f(x)=\sum_{n=-\infty}^{\infty}c_n\exp\left(\mathrm{i}\frac{2\pi n}{T}x\right), \tag{18}$$

$$c_n=\frac{1}{T}\int_{-T/2}^{T/2}f(x)\exp\left(-\mathrm{i}\frac{2\pi n}{T}x\right)\mathrm{d}x,\quad (n=0,\pm1,\pm2,\ldots). \tag{19}$$

In consideration of computation time, n cannot be infinite. So the $2M+1$ term approximation is

$$f(x)\approx\sum_{n=-M}^{M}c_n\exp\left(\mathrm{i}\frac{2\pi n}{T}x\right), \tag{20}$$

$$c_n=\begin{cases}\dfrac{D}{T}, & (n=0),\\ \dfrac{2}{\pi n}\sin\left(\dfrac{\pi nD}{T}\right), & (n=\pm1,\pm2,\ldots\pm M).\end{cases} \tag{21}$$

As $\pi n'D/T=(k+1/2)\pi$ $(k=0,1,2,\ldots)$, that is, $n'=T/D(k+1/2)$ $(k=0,1,2,\ldots)$, c'_n attains an extreme value,

$$\left|\frac{c'_n}{c_0}\right|=\frac{2}{\pi^2(k+1/2)}=\frac{2}{\pi^2}\frac{1}{n'T_\mathrm{r}}\approx\frac{2}{\pi^2}\frac{1}{MT_\mathrm{r}}. \tag{22}$$

From Eq. (22), $|c'_n/c_0|$ is inversely proportional to the product of width–period ratio and truncation constant. Meanwhile, the calculation error increases as $|c'_n/c_0|$ goes up. So the width–period ratio and truncation constant must be chosen reasonably.

Two assumptions are put forward. The one is that the physical model approximates to the nonperiod repaired pit as $T_\mathrm{r}\le0.2$, because the KDP crystal component is fine. Another is that the error of $2M+1$ term approximation satisfies the requirement as $|c'_n/c_0|\le0.1$.

In actual computation, the width–period ratio and truncation constant are 0.1 and 80 respectively, which meet the two assumptions above.

3. Result and discussion

3.1. Verification of physical model

In order to verify the physical model, a semicircular repaired pit on the surface of KDP crystal is assumed, whose diameter is 6 μm. The incident light wave is along the positive direction of z axis, and the wavelength (λ) is 1.064 μm. The thickness of KDP crystal component is 10 mm. Meanwhile, the repaired layer and substrate layer are divided into 300 layers and 100 layers respectively. The width–period ratio and truncation constant are 0.1 and 80 respectively. The light intensity inside KDP crystal is expressed by the relative light intensity.

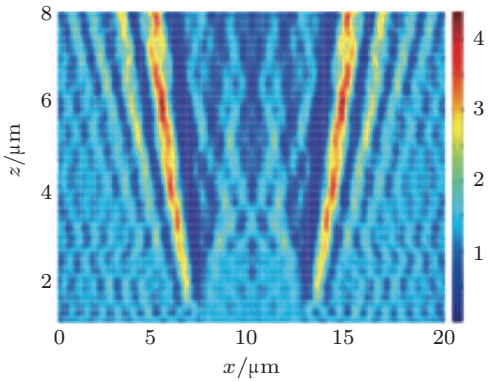


Fig. 4. (color online) Light intensity distribution after the modulation of a semicircular pit.

After calculation, the light intensity modulation inside crystal is shown in Fig. 4. This is consistent with the result obtained by the FDTD.[11,18] Therefore, the width–period ratio and truncation constant are reasonable, and the physical model built by Fourier model method is correct.

3.2. Incident laser modulation of Gaussian repaired pit

Figure 5(a) shows that the Gaussian repaired pit on the surface of KDP crystal is irradiated by high energy laser beams. Because of reflection and refraction of the laser from the surface of repaired pit, a certain light intensity enhanced region is formed inside the crystal. And the high energy concentration can cause damage to the crystal. As the width of Gaussian repaired pit is 120 μm and the depth is 20 μm,

the light intensity distribution inside KDP crystal is shown in Fig. 5(b).

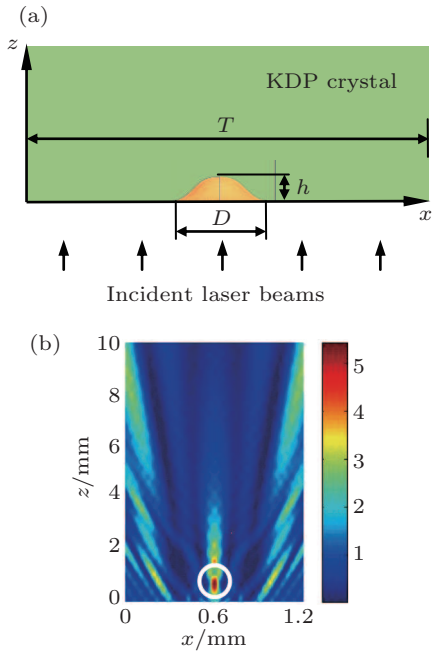


Fig. 5. (color online) (a) Schematic diagram of Gaussian repaired pit. (b) Light intensity distribution after modulation of Gaussian repaired pit.

The distribution of light intensity enhanced regions inside the crystal is similar to the letter 'W' shape. Due to the self-focusing effect near the repaired pit, the high energy is gathered and the maximum relative light intensity reaches 6.3, which easily causes the expansion of new damage inside the crystal. On the two sides of the repaired pit, the energy-enhanced regions expand gradually and expand into both sides. There is a large area of low light intensity region, far from the repaired pit, inside the crystal where new damage cannot appear. Meanwhile, due to the high energy-enhanced region in the middle of the crystal, it is easy to cause new body damage.

3.3. Modulation property of the width of Gaussian repaired pit

In order to study the relationship between the light intensity distribution within the crystal and the width of the Gaussian repair pit, the physical models with different widths are calculated. Since the depth of actual initial defect on the surface of KDP crystal is generally less than 20 μm,[12] the physical model with two different depths are chosen in calculation, namely 10 μm and 20 μm. As the depth is in this range, the change of maximum light intensity inside KDP crystal is not obvious. Figure 6 shows the modulation property curves with respect to width of the Gaussian repaired pit for given depths. For the different depths, the overall trend is that the maximum relative light intensity inside the crystal decreases constantly as the width of the Gaussian repaired pit increases.

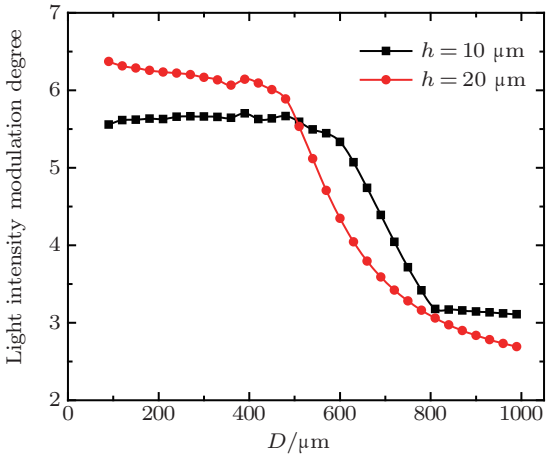


Fig. 6. (color online) Modulation property curves with respect to width of Gaussian repaired pit for given depths. The values of depth h are equal to 10 μm and 20 μm respectively.

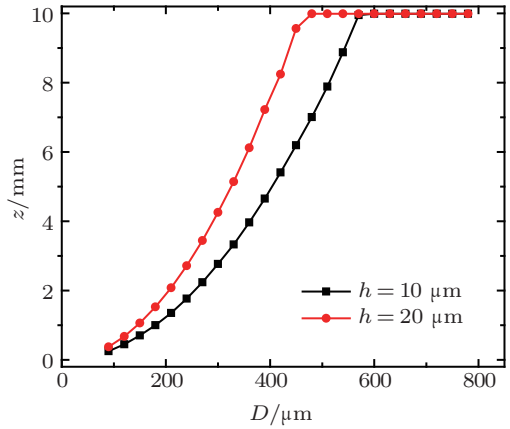


Fig. 7. (color online) Maximum intensity position curves with respect to width of Gaussian repaired pit for given depth values. The values of depth h are equal to 10 μm and 20 μm respectively.

As the width value of repaired pit varies between 100 μm–500 μm for the depth value of 20 μm, the maximum relative light intensity inside the crystal is high, and its value decreases slightly, which is likely to cause new damage within the crystal. However, for the repaired pit with 10 μm in depth, the maximum relative intensity inside crystal remains unchanged, this value is lower than that of the depth value of 20 μm, but it is still high. As the width value of repaired pit changes between 500 μm–800 μm, the maximum relative intensity inside the crystal decreases rapidly, and its value falls by nearly half. Then, this phenomenon can be explained. In Fig. 5(b), the maximum light intensity region (white circle region) near the front surface of the crystal is defined as the dangerous intensity region. Figure 7 shows that the position of the dangerous intensity region moves to the rear surface of the crystal gradually as the width value of repaired pit increases. When the width value exceeds 500 μm, the dangerous intensity region moves out of the crystal gradually, then its influence on the maximum light intensity within the crystal becomes smaller, so the maximum light intensity

declines sharply. As the width value of repaired pit is more than 800 μm, the maximum relative light intensity inside the crystal decreases relatively slowly. In short, the Gaussian repaired pit with high depth can alleviate the concentration of high energy inside the crystal well, which can improve the laser damage resistance.

As the positions of the maximum light intensity region are different in the z direction, the damages with different forms could appear. If the maximum light intensity concentrates inside the crystal, it could result in the bulk damage. In the case where the maximum light intensity focuses on the front or rear surface, surface damage could occur. Body damages are difficult to repair by mechanical method but surface damages are not, therefore the maximum light intensity is made to be located on the surface of crystal as much as possible. Figure 7 shows the variations of the position of the maximum light intensity inside the crystal with the width value of Gaussian repaired pit for the two different depths. As the width value of repaired pit changes between 100 μm–500 μm, the position of the maximum light intensity moves from the front surface (incident surface) to the back surface of the crystal gradually. As the width is more than 500 μm, the position of the maximum light intensity is near the surface of the crystal. For the Gaussian repaired pits with 200 μm–400 μm in depth, the position of the maximum light intensity is far from the surface of KDP crystal, which is easy to cause body damage, so the parameters in this interval should not be chosen.

4. Experiment

4.1. Machining of Gaussian repaired pit

In the experiment, a small precise five-axis machine tool,[19] built by our laboratory, is used to fabricate the Gaussian repaired pits. The overall structure of the machine tool with a size of 580 mm×500 mm×770 mm is shown in Fig. 8(a). In order to absorb the vibration and improve the machining accuracy of the machine tool, the base and the gantry are made of granite materials. The clamping is mounted on the second rotation axis (C-axis), so the crystal sample piece can linearly move along the X-axis and Y-axis directions and rotate about the Z axis. For the purpose of balancing the weight of the load to ensure that the force of Z-axis linear unit is within a rated range, a counterweight system is installed on the back of the machine tool. Meanwhile, in order to preset the cutter quickly and accurately and monitor the process, a CCD monitoring device is equipped on the machine tool. In the micro-milling process, the 0.05 mm∼0.8 mm diameter micro-tool is selected generally. In order to achieve a high linear velocity, the spindle speed must be high, and the maximum speed of the spindle adopted in the machine tool is 8×10^4 rpm.

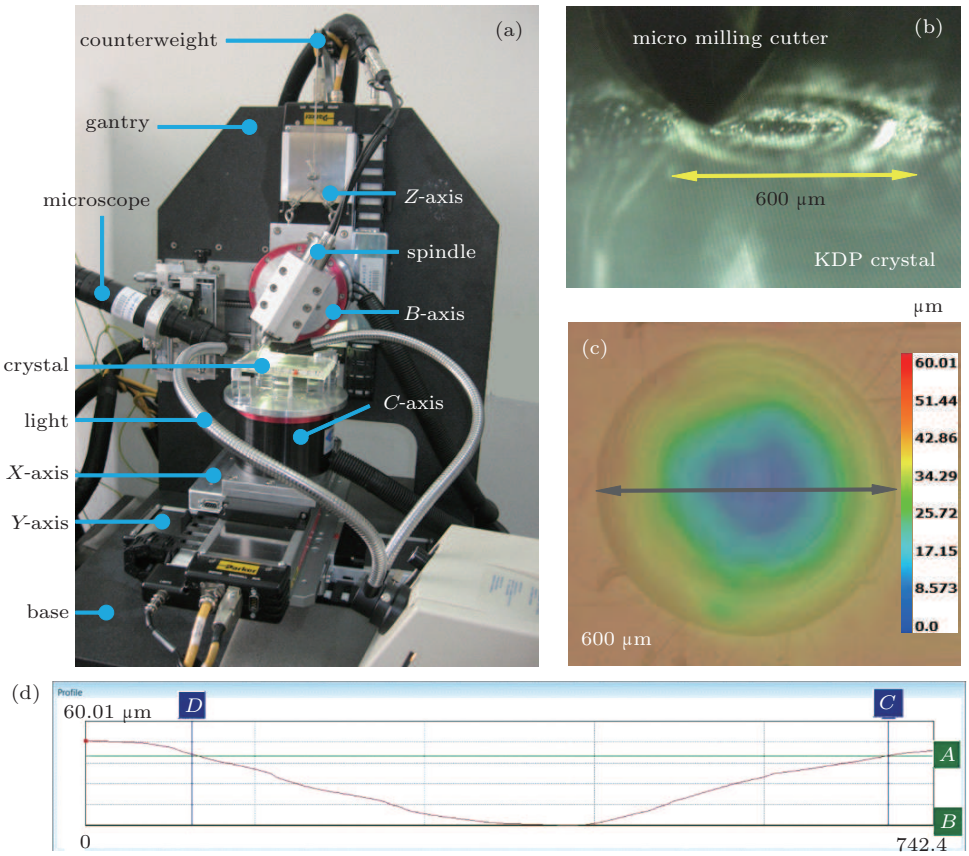


Fig. 8. (color online) The processing of Gaussian repaired pits by the micro-precise five-axis machine tool: (a) structure of machine tool; (b) machining process monitoring; (c) optical microscopy photograph of Gaussian repaired pit; (d) measured curve of cross section.

During processing, Gaussian surface is layered equally, and the thickness value of each layer is 1 μm. For each layer, the cutting path consists of concentric circles outward expanding from center as shown in Fig. 9.

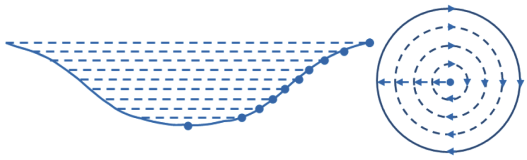


Fig. 9. (color online) Cutting path of Gaussian repaired pit during processing.

Because KDP crystal is a kind of soft brittle material, improper processing parameters can easily lead to a brittle cutting state for KDP crystal, which is bad for the processing quality.[20] So the processing parameters must be selected reasonably. The micro-milling parameters are shown in Table 1, the Gaussian repaired pits with three different widths (600 μm, 800 μm, and 1000 μm) and 20 μm in depth are processed on the surface of KDP crystal sample piece. After processing, an ultra-depth three-dimensional microscope (VHX 1000E) is used to observe the surface of Gaussian repaired pits. Figure 8(c) shows the 3D graph of Gaussian repaired pit with 600 μm, and the surface of the repaired pit presents a completely ductile cutting state. As shown in Fig. 8(d), the cross section of Gaussian repaired pit is measured by the super-depth microscope.

Table 1. Processing parameters of Gaussian repaired pits with micro-milling.

Tool radius R/mm	Step /μm	Feed f/(mm/min)	Milling depth a_p/μm	Spindle speed n/(10^4 rpm)	spindle deflection α /(°)
0.4	80	50	1	6	30

4.2. LIDT testing of Gaussian repaired pit

In order to test the ability of Gaussian repaired pits to improve laser damage resistance, laser irradiation experiments are made on the Gaussian repaired pits on the surface of KDP crystal sample piece. Figure 10 shows the optical path diagram of measuring laser-induced damage threshold. The laser used in the experiment is Nd:YGA laser produced by THALES LASER company, which can output a stable TEM_{00} mode laser with 355-nm wavelength. Actually, body damages appear easily inside KDP crystal. Therefore, in order to make surface damage first occur, the short-focus lens is used in the experiment. The spot at the back of focus irradiates the KDP crystal sample piece, so that the energy density on the surface of KDP crystal is greater than that inside the crystal. Moreover, the laser light beams generated by an He–Ne laser are collimated laser beams, and they can also be used to observe the initial damage by the light scattering at small angles inside KDP crystal sample piece. The Gaussian repaired pits on the surface of sample piece are found by a microscope, which can also be used to observe the damage.

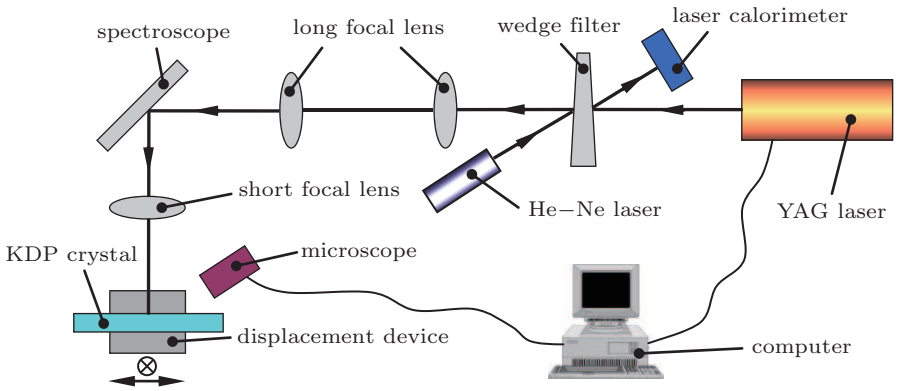


Fig. 10. (color online) Schematic diagram of measuring laser-induced damage threshold.

Parameters of the laser beam path system and environmental parameters are shown in Table 2. The R-on-1 mode is taken to measure laser damage threshold of the Gaussian repaired pits on KDP crystal sample piece. As the size of laser spot is smaller than that of repaired pit, the method of scanning irradiation is used for improving the test accuracy. Initially, a lower energy laser is selected to irradiate the repaired pit region twice with the scanning mode. If no damage occurs, the laser energy is increased, and scanning irradiation is done again. And so forth, until damage appears, the highest energy above which the damage will occur is taken as the laser damage threshold of Gaussian repaired pit.

Table 2. Experimental parameters used in laser damage test on KDP sample.

Parameters of the laser beam path system					Environmental parameters		
Pulse width/ns	Wavelength λ/nm	Repetition rate/Hz	Focal area A/mm^2	Incident angle/(°)	Vacuum state	Temperature/°C	Moisture/%
6	355	1	0.16	0	atmosphere	20–23	42

Figure 11 shows the measurements of laser damage threshold for different repaired pits. For comparison, laser damage threshold of the initial damage point is also measured. The laser damage thresholds of three kinds of Gaussian repaired pits (3.12 J/cm^2) are all higher than that of the initial damage point (1.95 J/cm^2), and the highest laser damage threshold of Gaussian repaired pits is beyond about 60% of the initial damage point. So the Gaussian repaired pit can improve the laser damage resistance of KDP crystal significantly. Meanwhile, as the width of the Gaussian repaired pit increases, the laser damage threshold goes up. The result indicates that the Gaussian repaired pit with larger width can better alleviate growth of the laser damage, which is consistent with the previous theoretical analysis.

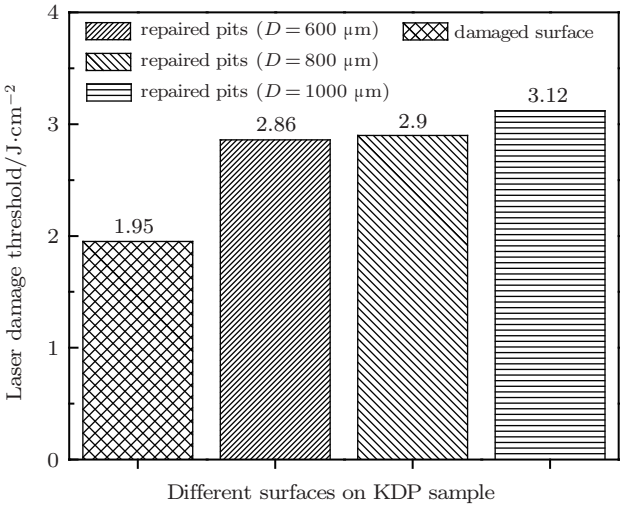


Fig. 11. Comparison of measured LIDTs for KDP crystal with initial damaged surface and Gaussian repaired pits of different depths.

Preliminary experiments demonstrate that the method of micro-mechanical repairing can improve the laser damage resistance of KDP crystal. However, there is a certain difference between the laser damage threshold of Gaussian repaired pits from the experiment and the laser damage threshold of perfect surface of KDP crystal, which probably relates to the micro-milling parameters, tool wearing, position accuracy of machine tool, etc. In order to further improve the laser damage resistance of repaired pits, the intrinsic links between repaired pits and the laser damage threshold of KDP crystal should be studied in depth.

5. Conclusion

This paper studies how the Gaussian repaired pits with different values of width and depth affect the light intensity modulation inside the KDP crystal by Fourier model method. The conclusions are as follows.

(i) Fourier model method can be used in the light intensity modulation of Gaussian repaired pit. The computing error is inversely proportional to the product of the width–period ratio of repaired pit and the truncation constant.

(ii) After analyzing the calculation results about the physical model of Gaussian repaired pits, it is found that the maximum light intensity inside KDP crystal decreases as the width value of Gaussian repaired pit increases, but the maximum light intensity is not sensitive to the variation of the depth value of Gaussian repaired pit as the depth is less than 20 μm.

(iii) The laser damage threshold of Gaussian repaired pits with different width values produced by micro-milling method is tested experimentally, the results demonstrate that the Gaussian repaired pits can obviously improve the laser damage resistance of KDP crystal, and the laser damage threshold of repaired pit goes up with increasing the width value.

References

[1] Keefe D 1982 *Ann. Rev. Nucl. Part. Sci.* **32** 391
[2] Lindl J D, McCrory R L and Campbell E M 1992 *Phys. Today* **45** 22
[3] Sasaki T and Yokotani A 1990 *J. Cryst. Growth* **99** 820
[4] Fujioka K, Matsuo S, Kanabe T, Fujita H and Nakatsuka M 1997 *J. Cryst. Growth* **181** 265
[5] Zaitseva N, Atherton J, Rozsa R, Carman L, Smolsky I, Runkel M, Ryon R and James L 1999 *J. Cryst. Growth* **197** 911
[6] Xu Q, Wang J, Li W and Zeng X 1999 *Proc. SPIE* **3862** 236
[7] Yoshida H, Jitsuno T, Fujita H, Nakatsuka M, Yoshimura M, Sasaki T and Yoshida K 2000 *Appl. Phys. B* **70** 195
[8] Guillet F, Bertussi B, Lamaignere L, Leborgne X and Minot B 2007 *Proc. SPIE* **6720** 672008
[9] Geraghty P, Carr W, Draggoo V, Hackel R, Mailhiot C and Norton M 2006 *Proc. SPIE* **6403** 64030Q
[10] Li M Q, Chen M J, An C H, Zhou L, Cheng J, Xiao Y and Jiang W 2012 *Chin. Phys. B* **21** 050301
[11] Chen M J, Cheng J, Li M Q and Xiao Y 2012 *Chin. Phys. B* **21** 064212
[12] Carr C W, Matthews M J, Bude J D and Spaeth M L 2006 *Proc. SPIE* **6403** 64030K
[13] Li L F 1996 *J. Opt. Soc. Am. A* **13** 1870
[14] Zhou C H and Li L F 2004 *J. Opt. A* **6** 43
[15] Bai B F and Li L F 2006 *Opt. Common.* **262** 140
[16] Fu K X, Zhang D Y, Wang Z H, Zhang Q Z and Zhang J 1998 *Acta Phys. Sin.* **47** 1278 (in Chinese)
[17] Ma J Y, Liu S J, Jin Y X, Xu C, Shao J D and Fan Z X 2008 *Opt. Commun.* **281** 3295
[18] Zhang L, Huang L, Fan S J, Bai G X, Li K F, Chen W and Hu L L 2010 *Appl. Opt.* **49** 6668
[19] Xiao Y, Chen M J, Chu X and Tian W L 2013 *Int. J. Adv. Manuf. Tech.* **67** 387
[20] Peng Y F, Guo Y B and Xu Q 2009 *Proc. SPIE* **7282** 72820S